J. Fac. Pharm. Ankara / Ankara Ecz. Fak. Derg., 48(2): 513-524, 2024
Doi: 10.33483/jfpau.1380350

ORIGINAL ARTICLE / ÖZGÜN MAKALE

IN SILICO APPROACHES ON PHENYLALANINE HYDROXYLASE INHIBITOR-RELATED COMPOUNDS USED IN PARKINSON'S DISEASE TREATMENT

PARKİNSON HASTALIĞI TEDAVİSİNDE KULLANILAN FENİLALANİN HİDROKSİLAZ İNHİBİTÖRÜ İLE İLİŞKİLİ BİLEŞİKLERE İLİŞKİN İN SİLİKO YAKLAŞIMLAR

Hatice AKKAYA[1]*, Engin SÜMER[2]

[1]Health Sciences University, Faculty of Pharmacy, Department of Biochemistry, 34668, Istanbul, Türkiye
[2]Yeditepe University, Faculty of Medicine, Experimental Research Center, 34755, Istanbul, Türkiye

ABSTRACT

Objective: *In Parkinson's disease, Levodopa with Carbidopa addresses dopamine deficiency. Phenylalanine hydroxylase catalyzes phenylalanine to tyrosine conversion crucial for dopamine synthesis. Inhibiting phenylalanine hydroxylase may enhance Carbidopa's effects, preventing peripheral dopamine synthesis. The study used virtual scanning, molecular docking, and dynamics simulation to explore phenylalanine hydroxylase interactions with Carbidopa and similar ligands. ADME/T assessments and drug similarity tests were conducted to evaluate therapeutic potential in biological systems.*
Material and Method: *A molecular docking study was performed on the structures obtained from the PubChem database and human PAH (PDB ID: 6PAH) using Autodock Vina within Chimera 1.16. Furthermore, the ligands underwent ADME/T assays, which are crucial aspects in drug development.*
Result and Discussion: *The study suggests that 2-(2-Aminohydrazinyl)-3-(3,4-dihydroxyphenyl)-2-methylpropanoic acid shows promise as a phenylalanine hydroxylase inhibitor for Parkinson's disease treatment, but further research is needed to assess its safety, efficacy, and specificity, particularly in extracerebral regions, while also exploring its potential to improve the effectiveness of Levadopa/Carbidopa combination therapy.*
Keywords: *Drug development, inhibitor, in silico, Parkinson's disease, phenylalanine hydroxylase*

ÖZ

Amaç: *Parkinson hastalığında, Levodopa ile Carbidopa kullanılarak dopamin eksikliği ele alınır. Fenilalanin hidroksilaz, dopamin sentezi için önemli olan fenilalanin'in tirozin'e dönüşümünü katalizler. Fenilalanin hidroksilaz'ın inhibe edilmesi, periferik dopamin sentezini engelleyerek Carbidopa'nın etkilerini artırabilir. Çalışmada, fenilalanin hidroksilazın Carbidopa ve benzeri ligandlarla etkileşimlerini araştırmak için sanal tarama, moleküler bağlanma ve dinamik simulasyon kullanıldı. ADME/T değerlendirmeleri ve ilaç benzerlik testleri biyolojik sistemlerdeki terapötik potansiyeli değerlendirmek amacıyla yapıldı.*
Gereç ve Yöntem: *PubChem veritabanından elde edilen yapılar ve insan fenialanin hidroksilaz (PDB Kimlik Numarası: 6PAH) üzerinde bir moleküler bağlanma çalışması, Autodock Vina'nın Chimera 1.16 içinde kullanılarak gerçekleştirildi. Ayrıca, ligandlar ilaç geliştirme sürecinde önemli bir aşama olan ADME/T analizlerine tabi tutuldu.*

* **Corresponding Author / Sorumlu Yazar:** Hatice Akkaya
e-mail / e-posta: hatice.akkaya@sbu.edu.tr, **Phone / Tel.:** +902167778777

Submitted / Gönderilme : 23.10.2023
Accepted / Kabul : 03.03.2024
Published / Yayınlanma : 20.05.2024

Sonuç ve Tartışma: *Çalışma, 2-(2-Aminohydrazinyl)-3-(3,4-dihydroxyphenyl)-2-methylpropanoic acid'in Parkinson hastalığının tedavisinde fenilalanin hidroksilaz inhibitörü olarak umut vadettiğini öne sürüyor. Ancak, özellikle ekstraserebral bölgelerde güvenlik, etkinlik ve özgünlük değerlendirmek için daha fazla araştırmaya ihtiyaç olduğunu ve aynı zamanda Levadopa/Carbidopa kombinasyon tedavisinin etkinliğini artırma potansiyelini keşfetmenin önemli olduğunu belirtiyor.*
Anahtar Kelimeler: *Fenilalanin hidroksilaz, ilaç geliştirme, inhibitör, in siliko, Parkinson hastalığı*

INTRODUCTION

Alzheimer's disease (AD) stands as the most prevalent neurodegenerative disease globally [1], with Parkinson's disease (PD) following closely behind [2]. The disease is characterized by the degeneration of dopamine neurons, leading to dopamine deficiency, which is the major deficit underlying PD. The reduction in dopamine levels eventually produces motor symptoms, such as bradykinesia and akinesia [3]. Although various pharmacological treatments, such as the use of dopamine agonists and monoamine oxidase inhibitors, have been effective in alleviating the disease symptoms, treatment with 3,4-dihydroxyphenylalanine (levodopa, L-DOPA, or DAH), the precursor of dopamine, is currently the safest and most effective strategy [4,5]. However, the efficacy of this treatment is limited by the conversion of L-DOPA to dopamine in the extracerebral regions, reducing the bioavailability of L-DOPA in the brain. Thus, L-DOPA is commonly used in combination with Carbidopa, an inhibitor of DOPA decarboxylase (DDC), which inhibits the conversion of L-DOPA to dopamine in the periphery owing to its inability to cross the blood-brain barrier (BBB) [6,7]. This increases the amount of L-DOPA reaching the brain, where it can be converted to dopamine to relieve symptoms associated with PD.

The diagnosis and treatment of Parkinson's disease emphasize the importance of carbidopa-levodopa formulations, often used alongside other medications [8]. Advanced treatments such as deep brain stimulation and levodopa-carbidopa enteral suspension help manage medication-resistant symptoms [9]. Despite the initially promising effects of dual L-DOPA/Carbidopa therapy, in recent years, frequent fluctuations in dopamine levels have become an issue [10]. While the underlying reasons remain to be elucidated, several measures have been taken to compensate for these fluctuations [11]. including repeated L-DOPA intake or switching to gel-based from oral applications. However, despite their effectiveness in managing symptoms, levodopa-carbidopa therapy has several shortcomings and limitations. One major limitation is the development of motor fluctuations, where patients experience alternating periods of increased mobility (on periods) and worsened symptoms (off periods), significantly affecting their quality of life [12,13]. Long-term use can lead to the development of levodopa-induced dyskinesias (LIDs) [14], involuntary movements that worsen over time. Additionally, while levodopa-carbidopa effectively addresses motor symptoms, it may have limited efficacy in managing non-motor symptoms such as cognitive impairment, psychiatric symptoms, and sleep disturbances. Furthermore, levodopa-carbidopa primarily provides symptomatic relief and does not alter the underlying disease progression in Parkinson's disease. Therefore, the recommended L-DOPA dose of 400 mg/day should not be exceeded [8,15].

Coupling the existing treatments with the targeting of other steps in the dopamine synthesis pathway might be an effective strategy to reduce peripheral L-DOPA levels during PD therapy.

The enzyme phenylalanine hydroxylase (PAH) (EC 1.14.16.1) converts L-phenylalanine into L-tyrosine, which is then hydroxylated to form L-DOPA by the enzyme Tyrosine hydroxylase (TH) [16,17]. These tetrameric enzymes consist of regulatory N-terminal domains, catalytic domains with structural similarity, and C-terminal domains responsible for oligomerization. This study initially explored Carbidopa's affinity to PAH's active site to understand its potential interference with L-DOPA synthesis. Next, chemicals structurally similar to Carbidopa were screened as ligands using molecular docking, a technique integrating computational approaches in drug design. Molecular dynamics simulation was then employed to further elucidate the binding mechanism and conformational behavior of the target protein and potential inhibitors [18,19,20,21], Additionally, the ligands underwent

ADME/T assays to assess their pharmacokinetics and safety profile, crucial in drug development [22,23].

MATERIAL AND METHOD

Virtual Screening and Selection of Target Protein and Ligands

L-DOPA is a catechol that can bind the Fe(III) at the active site of PAH, causing a reversible shift to the inactive form of the enzyme. The crystallographic structure of L-DOPA-bound 6PAH was downloaded from the Protein Data Bank. Carbidopa (A) and structurally similar 3-(3,4-Dihydroxyphenyl)-2-hydrazinylpropanoic acid (B), 3-(3,4-Dihydroxyphenyl)-2-hydrazinyl-2-methyl propanoate (C), 6-[3-(3,4-Dihydroxyphenyl)-2-hydrazinyl-2-methylpropanoyl]oxyhexanoic acid (D), Ethyl 3-(3,4-dihydroxyphenyl)-2-hydrazinyl-2-methylpropanoate (Carbidopa Ethyl Ester) (E), 2-(2-aminohydrazinyl)-3-(3,4-dihydroxyphenyl)-2-methylpropanoic acid (F), and 2-[(3,4-dihydroxy phenyl)methyl]-2-hydrazinylbutanoic acid (G) were selected as ligands.

Preparation of Protein Structure and Ligands

The target protein PDB file was obtained [24-26], ligands (small molecules) and water molecules attached to the protein structure were deleted from the 3D crystallographic structure, and the final protein structure was saved as a Mol2 file by adding polar hydrogen atoms and charges. SMILES notations were copied from the PubChem database. Energy minimization was achieved using the Build Structure tool embedded in Chimera. Ligands were saved in Mol2 file for docking.

Final Docking with Autodock Vina Embedded in Chimera (1.16)

The ligand molecule was imported in PDBQT format into the output file. AutoDock Vina command prompt was run by entering the previously determined active site coordinates, and the results were analyzed [18].

Grid Box Preparation

The active site of DAH bound to 6PAH in its crystallographic structure was identified by taking the arithmetic average of the x, y, and z coordinates of DAH (Table 1). The search area for the grid box was taken as 30 × 30 × 30 Å [26].

Table 1. Coordinate calculation for the 6PAH-bound DAH ligand

Residue Name (RES)	Chain Identifier (C)	Sequence Number Insertion Code (SSEQI)	x	y	z	Resolution	B-factor	Atom
DAH	A	600	-7.111	27.750	4.352	1.00	56.41	N
DAH	A	600	-7.194	26.678	3.307	1.00	56.32	C
DAH	A	600	-8.666	26.319	2.931	1.00	56.53	C
DAH	A	600	-8.977	25.836	1.814	1.00	56.42	O
DAH	A	600	-6.300	25.430	3.605	1.00	55.47	C
DAH	A	600	-5.066	25.551	4.533	1.00	54.66	C
DAH	A	600	-5.196	26.087	5.871	1.00	54.32	C
DAH	A	600	-3.783	25.126	4.068	1.00	53.88	C
DAH	A	600	-4.066	26.186	6.716	1.00	53.73	C
DAH	A	600	-2.645	25.223	4.912	1.00	53.38	C
DAH	A	600	-2.787	25.760	6.259	1.00	53.40	C
DAH	A	600	-1.435	24.795	4.426	1.00	52.27	O
DAH	A	600	-1.708	25.875	7.121	1.00	52.85	O
DAH	A	600	-9.580	26.579	3.957	1.00	57.03	O

The arithmetic mean of the x, y, and z coordinates is respectively -5.322, 25.943, and 4.562.

Computer-Based Analysis of Pharmacokinetics and Drug-likeness

Drug similarity as well as oral bioavailability (Lipinski's rule of 5) [27] and safety profile of the compounds selected as drug candidates were evaluated with ADME/T (http://www.swissadme.ch/, http://lmmd.ecust.edu.cn/admetsar2) which are used especially to estimate pharmacokinetic properties.

Software Used

Windows 10 Microsoft operating system was installed. The UCSF Chimera (1.16) program (https://www.cgl.ucsf.edu/chimera/download.html) was run for docking with AutoDock Vina [18], hosted by The Scripps Research Institute (USA), frequently used for molecular docking simulations [28,29]. Protein Data Bank (https://www.rcsb.org/) and PubChem were searched for protein and chemical (ligand) structures, respectively. IGemDOCK V2.1 was used for the elimination of ligands by pre-scoring. Plip-tool (https://plip-tool.biotec.tu-dresden.de/plip-web/plip/index) [30] and the ProteinsPlus web server (https://proteins.plus/) were used to analyze the bonds and distances between the target protein and selected ligands. The iMod server package (https://imods.iqfr.csic.es/) was used for modeling, image processing, and 2D and 3D data analyses [31]. The ligands were subjected to ADME/T assays to evaluate their pharmacokinetics and safety profile, which are vital aspects in drug development. (http://www.swissadme.ch/, http://lmmd.ecust.edu.cn/admetsar2)

RESULT AND DISCUSSION

This *in silico* structure-based study conducted to predict ligand-target interactions [32] revealed proteins that are structurally similar to DAH, which might interact with PAH (Figure 1).

Figure 1. The crystal structure of human 6PAH

The surface of a protein presents a distribution of charge and hydrophobicity that enables interactions with suitable surfaces [33,34] and influences the conformational stability of the protein structure. Surface properties also affect interactions with other biomolecules, which can contribute to the modification of a protein's behavior and stability, affecting its bioactivity [35]. In this respect, hydrogen bonding (at positions G131, L133, Y209, and E214) and hydrophobic interactions (at V129, F138, and P165) play important roles in the binding of the donepezil ligand to human PAH (Figure 2).

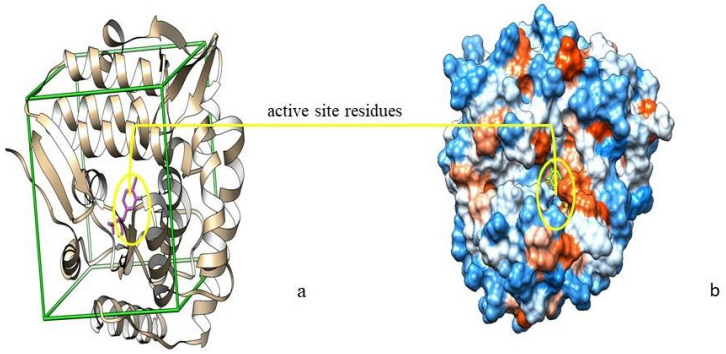

Figure 2. Visualization of a) the protein structure and b) surface hydrophobicity with active site residues in the crystal structure of 6PAH

The predicted binding affinities are given in kcal/mol. Root mean square deviation (RMSD) values are computed using the optimal mode as the basis. The difference between the rmsd/lb (RMSD lower bound) and rmsd/ub (RMSD upper bound) metrics is determined by how atoms are matched in the distance calculation. The ligands (Table 2) were pre-screened using the Igemdock software. The binding energies of ligands are shown in Table 3. L-DOPA (DAH) is found as a complex in the crystal structure of recombinant human PAH.

Table 2. Structures of the ligands obtained from PubChem

Structure	Ligand	PubChem ID
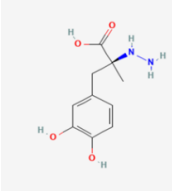	L-alpha-methyldopa hydrazine (Carbidopa) (A)	CID: 34359
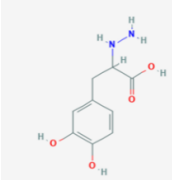	3-(3,4-Dihydroxyphenyl)-2-hydrazinylpropanoic acid (B)	CID: 13687898
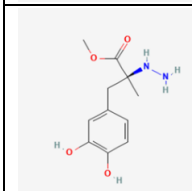	3-(3,4-Dihydroxyphenyl)-2-hydrazinyl-2-methylpropanoate (C)	CID: 21964612
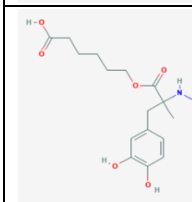	6-[3-(3,4-Dihydroxyphenyl)-2-hydrazinyl-2-methylpropanoyl]oxyhexanoic acid (D)	CID: 21964631
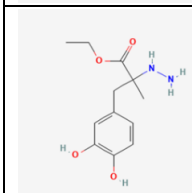	Ethyl 3-(3,4-dihydroxyphenyl)-2-hydrazinyl-2-methyl-propanoate (Carbidopa Ethyl Ester) (E)	CID: 21964632
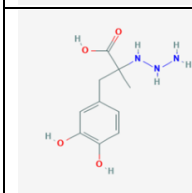	2-(2-Aminohydrazinyl)-3-(3,4-dihydroxyphenyl)-2-methyl propanoic acid (F)	CID: 22234765
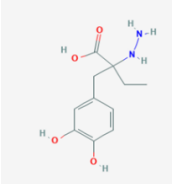	2-[(3,4-Dihydroxyphenyl)methyl]-2-hydrazinylbutanoic acid (G)	CID: 53679931

Carbidopa (A), utilized alongside L-DOPA in PD therapy [7], and six structurally similar ligands (B), (C), (D), (E), (F), and (G) were positioned within the drug binding pocket of the human PAH enzyme (Table 2 and Figure 3, 4). The binding energies of the protein-ligand complexes obtained from molecular docking were compared with the RMSD values of the corresponding compounds (Table 3). Carbidopa (A) was chosen as the positive control due to its structural resemblance to DAH, and its comparison with the other six ligands confirmed their potential binding activity against PAH. The docking scores of the structures-B (-6.7 kcal/mol), C (-6.9 kcal/mol), D (-6.8 kcal/mol), E (-6.6 kcal/mol), F (-7.1 kcal/mol), and G (-6.6 kcal/mol)-were consistent. The binding energy was calculated as -92.03 kcal/mol for (B), -88.92 kcal/mol for (C), -99.58 kcal/mol for (D), -88.02 kcal/mol for (E), -100.45 kcal/mol for (F), and -89.96 kcal/mol for (G) (Table 3). These findings suggested that 2-(2-Aminohydrazinyl)-3-(3,4-dihydroxyphenyl)-2-methylpropanoic acid (F) is more effective in binding to PAH than all currently known and tested ligands. Detailed examination of the protein-ligand bonds revealed the presence of hydrogen bonds and hydrophobic interactions between all ligands and PAH, similar to the 6PAH-DAH complex. Additionally, π-stacking was observed in (B), and both π-stacking and salt bridges were formed in (E) and (F). Ligands were found to interact with 5 to 7 amino acid residues at the active site of 6PAH.

Table 3. Docking scores and binding energies of the ligands for PAH and RMSD values

Ligand molecules	Binding affinity (kcal/mol)	RMSD lower bound	RMSD upper bound	Binding energy (kcal/mol)
(A)	-6.7	1.974	2.325	-92.36
(B)	-6.7	3.962	5.859	-92.03
(C)	-6.9	2.540	3.819	-88.92
(D)	-6.8	9.163	11.938	-99.58
(E)	-6.6	1.656	2.351	-88.02
(F)	-7.1	9.191	10.781	-100.45
(G)	-6.6	8.941	11.111	-89.96

RMSD, root mean square deviation

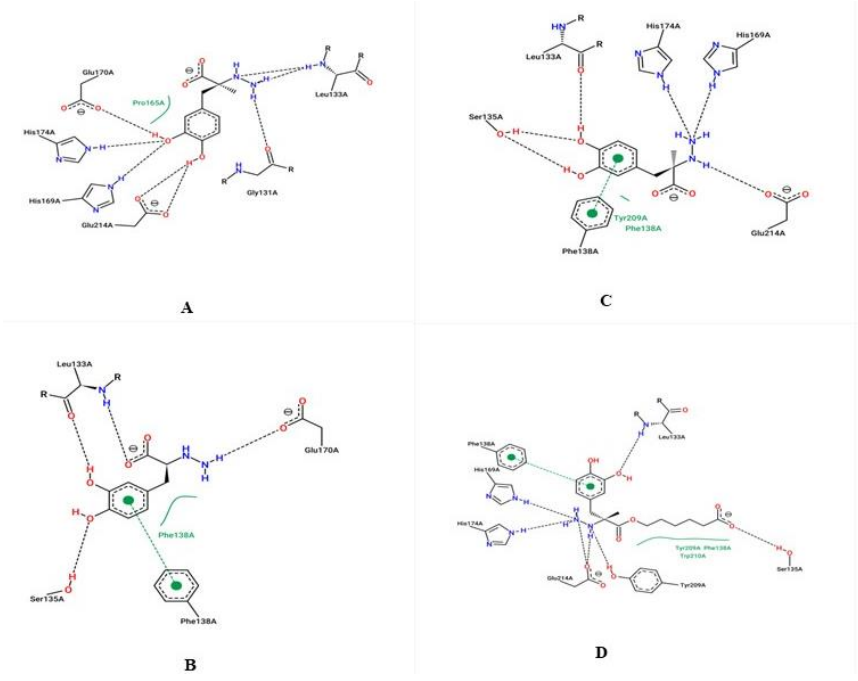

Figure 3. Interactions of target protein and the selected ligands (A, B, C, D). Protein-ligand interaction profiles are named by the letter of the respective ligand

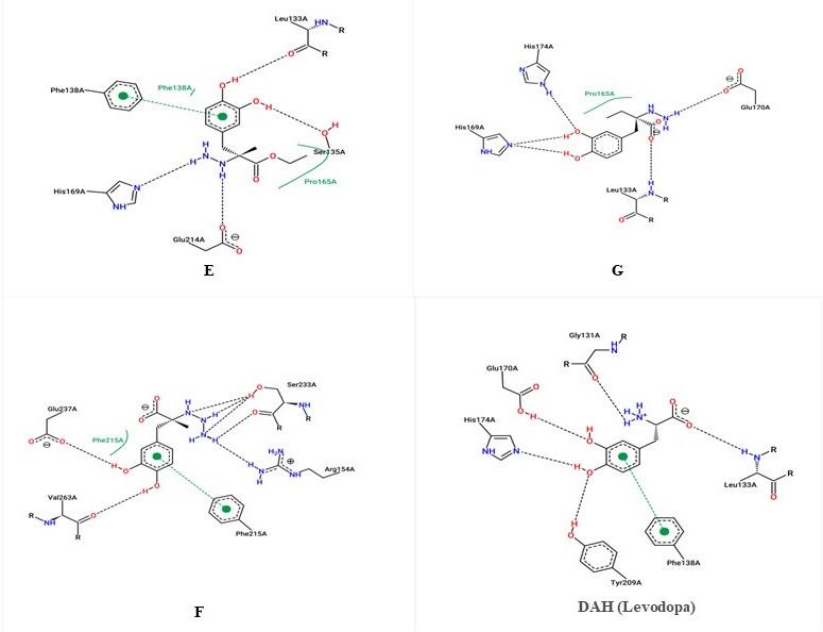

Figure 4. Interactions of target protein and the selected ligands (E, F, G). Protein-ligand interaction profiles are named by the letter of the respective ligand

L132, F138, and P165 hydrophobic interactions and G131, L133, and H169 hydrogen bonds were observed when Carbidopa (A) was bound to the PAH enzyme. L133, S135, and H148 hydrogen bonds, L132 and F138 hydrophobic interactions, and F138 π-stacking interactions were observed for (B). S135, H174, Y209, and G214 hydrogen bonds and L132, F138, and Q214 hydrophobic forces were found to contribute to the interaction between (C) and 6PAH. G131, L133, and Y209 hydrogen bonds and F138, P165, A206, T209, and W210 hydrophobic interactions were noted in our modeling for (D)-6PAH. S135 and Q214 hydrogen bonds, V129, L132, F138, and Y209 hydrophobic interactions, F138 π-stacking interactions, and H169 and H174 salt bridges were observed for (E)-6PAH. A154, S233, and G265 hydrogen bonds, F215 π-stacking interactions, and H169 salt bridges were noted in (F)-6PAH modeling. L133, H148, Y150, and H169 hydrogen bonds and L132, F138, and P165 hydrophobic forces played a role in the interaction between (G) and 6PAH. When the ligands were examined, the lowest hydrogen bond (H-A) distance was reported as 2.09 Å in positive control Carbidopa (A). Meanwhile, the lowest H-A values in the (F) ligand were found as 2.17 Å, 2.80 Å, 2.35 Å, and 2.78 Å. These results indicated that the binding between PAH and (F) may be stronger in comparison with the other ligands.

Protein's three-dimensional configuration is intricately shaped by a delicate interplay of weak forces, notably hydrogen bonds, salt bridges, and the hydrophobic effect, crucial for proper folding and structural integrity. Additionally, the cation-π interaction, an increasingly acknowledged non-covalent binding force in structural biology, has become more prominent. Both theoretical and experimental studies have demonstrated that cation-π interactions can be quite strong, both in the gas phase and in aqueous environments [36]. Therefore, the hydrogen bonds (with the shortest H-A distance), salt bridges, and π-stacking interactions present in the structure of 2-(2-Aminohydrazinyl)-3-(3,4-dihydroxyphenyl)-2-methylpropanoic acid ligand are crucial for determining the three-dimensional structure of proteins and are among the reasons why this ligand is preferred.

Flexibility is a crucial factor for protein-protein interactions or the interactions of biological macromolecules with their substrates [37]. The iMOD server was used to calculate the flexibility of the protein, as well as molecular motion [38]. The NMA study of the complex showed mobility and flexibility (Figure 5A). Deformability is associated with flexibility, and the B factor is associated with protein mobility [39]. The B factor graphs in Figure 5B represent the comparison between the NMA and PDB fields of the complex. The highly deformable regions of the (F)-6PAH complex are indicated by the highest peaks. Eigenvalue and variance plots (Figure 5C) of the (F)-6PAH complex showed an

inverse relationship with the normal mode. 4.709380e-0.4 is the eigenvalue of the complex calculated with the iMod server. The correlation between the residues of the (F)-6PAH complex is displayed by the covariance map. Blue, red, and white colors between residues in the matrix indicate anticorrelation, correlation, and uncorrelated motion, respectively (Figure 5-D). Interatomic relationships are shown in Figure 5E. Dark gray shows the stiffer parts; the covariance matrices and elastic maps gave reasonable values.

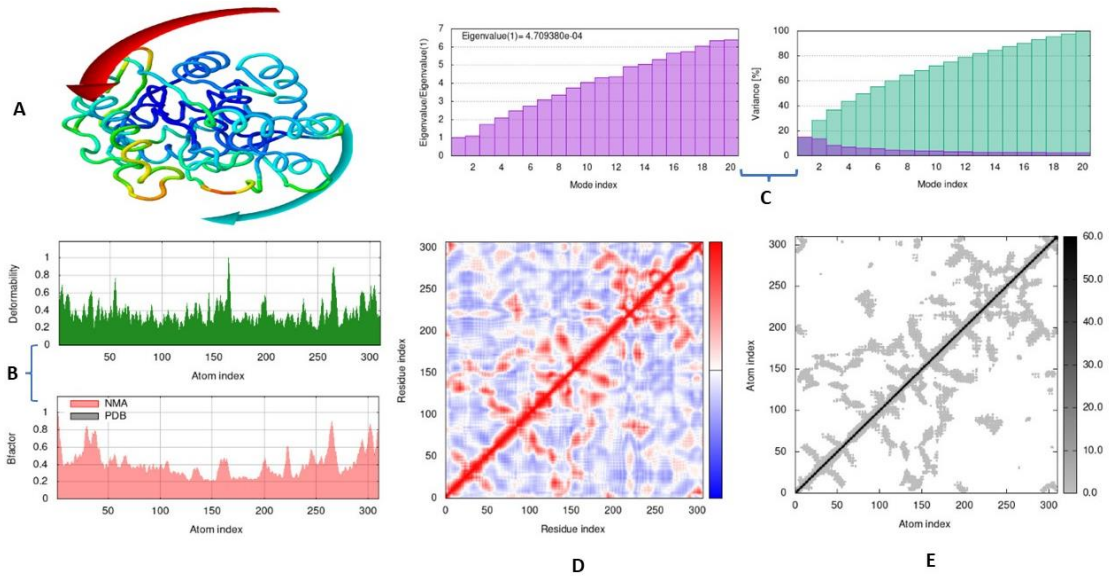

Figure 5. The results from molecular dynamics simulations in iMods pertain to the (F)-6PAH complex. A. Molecular mobility assessed by normal mode analysis (NMA) of the docked proteins. The colored affine arrows show the mobility. B. Deformability and the B-factor plot. C. Eigenvalue (left) and variance plots (right). The calculated eigenvalue is 4.709380e-0.4. In the variance plot D, cumulative variance is illustrated by the green-shaded bars, while individual variance is indicated by the purple-shaded bars. Covariance map. Blue, anticorrelation; red, correlation; white, uncorrelated motion. E. Elastic network model. Dark gray shows the stiffer parts

The exploration of the ADME properties of drugs using computer-based models and calculations is essential in the processes of drug development. Simultaneously, Lipinski's Rule of Five for Drug Molecules specifies that a potential drug candidate must adhere to four specific physical and chemical properties within acceptable limits to attain high oral bioavailability. [40]. According to Lipinski's rule of five, an orally active drug can have no more than one violation of these conditions [41]. When evaluating ligands that meet Lipinski criteria, the assessment of Carbidopa and ligands with similar structures as potential drug candidates was conducted using the SwissADME platform. According to the results, it was found that the log P values of all compounds were below 5, and the molecular weight of each compound was within the acceptable range (MW<500). The number of H-bond acceptors (≤10) and donors (≤5) also fell within acceptable limits. Only the F ligand showed 6 H-bond donors (Table 4). However, other pharmacokinetic and pharmacodynamic factors should also be considered. Seven compounds were identified within the topological polar surface area range (TPSA; <140). The number of rotatable bonds for all compounds was within the acceptable range (≤10) as shown in Table 4. When all ligands were evaluated in terms of lipophilicity (LIPO; -0.7<XlogP3<5), size (150<MW<500), polarity (20<TPSA<30), solubility (INSOLU, -6<log S<0), saturation (INSATU; 0.25<carbon fraction in sp3 hybridization<1), and flexibility (FLEX, 0<rotatable bonds<9), deviation was observed in saturation for ligand B (0.22) and in flexibility for ligand D (9). Other ligands are within the optimal range. The analysis results demonstrated that the five properties fell within the favorable range, categorizing the compound as a drug-like molecule. Except for compound D, the other ligands, especially ligands F and G, can be considered suitable for injectable administration as they are within

the appropriate flexibility range [42]. Additionally, when pharmacokinetic properties were evaluated, it was predicted that other ligands, like Carbidopa, did not cross the BBB. According to ADMET analysis, the acute oral toxicity of other ligands, like Carbidopa, is classified as Category III (slightly toxic). (Category III includes compounds with LD_{50} values greater than 500mg/kg but less than 5000mg/kg (http://lmmd.ecust.edu.cn/admetsar2) [43].

Table 4. List of pharmacokinetic properties of ligands

Properties	**Physicochemical properties**								**Lipophili-city**	**Water Solubility**	**Pharmaco-kinetics**	**Drug-likeness**	**Medicinal chemistry**
Parameters	Molecular weight (g/mol)	Number of heavy atoms	Number of aromatic heavy atoms	Number of rotatable bonds	Number of H-bond acceptors	Number of H-bond donors	Molar Refrac-tivity	TPSA (Å²)	Log Po/w	LogS (ESOL)	GI absorbtion/ BBB permeant	Lipinski/ violation	Synthetic accecibility
A	226.23	16	6	4	6	5	57.19	115.81	-2.17	0.11	High/No	Yes; 0 violation	2.25
B	212.20	15	6	4	6	5	52.35	115.81	-2.98	0.69	High/No	Yes; 0 violation	2.15
C	225.22	16	6	4	6	4	55.25	118.64	-2.17	0.12	High/No	Yes; 0 violation	2.21
D	340.37	24	6	11	8	5	87.32	142.11	-1.27	-0.61	Low/No	Yes; 0 violation	3.21
E	254.28	18	6	6	6	4	66.32	104.81	0.81	-1.78	High/No	Yes; 0 violation	2.66
F	241.24	17	6	5	6	6	60.00	127.84	-2.40	0.25	High/No	Yes; 1 violation: NHorOH>5	2.47
G	240.26	17	6	5	6	5	62.00	115.81	-1.64	-0.23	High/No	Yes; 0 violation	2.36

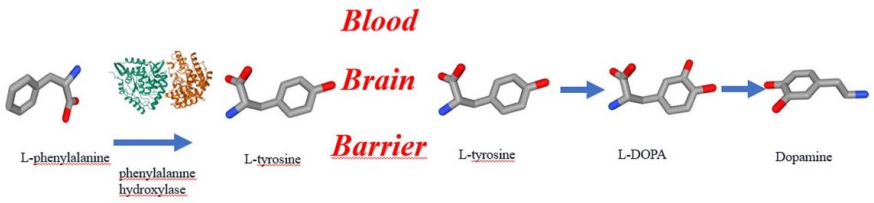

Figure 6. Phenylalanine tyrosine metabolic pathway

L-DOPA is widely used in Parkinson's's disease (PD) treatment, yet concerns persist about its fluctuating levels during prolonged therapy [44], with underlying reasons not fully understood [10]. These fluctuations may result from negative feedback due to L-DOPA binding with PAH. In physiological conditions, L-DOPA, derived from tyrosine conversion by TH activity (Figure 6), binds to the iron on PAH, temporarily shifting the enzyme to its inactive state and inhibiting L-DOPA synthesis [45]. During L-DOPA treatment, acute peripheral level increases may induce this negative feedback loop. Given the potential interference of normal pathway activity with appropriate dosage levels and intervals, targeting this pathway during PD therapy could be beneficial. Carbidopa, used with L-DOPA to decrease its conversion to dopamine in peripheral regions, shares structural similarities with L-DOPA. Our study found that carbidopa binds to PAH with a binding affinity of -6.87 kcal/mol and energy of -92.36 kcal/mol, potentially regulating L-DOPA levels. However, combination therapy stability in this aspect remains uncertain. Additionally, we identified 2-(2-Aminohydrazinyl)-3-(3,4-dihydroxyphenyl)-2-methylpropanoic acid as a promising PAH inhibitor, exhibiting improved activity with a binding affinity of -7.1 kcal/mol, energy of -100.45 kcal/mol, and favorable molecular dynamics. Most ligands were suitable for injectable administration, with carbidopa-like ligands predicted to have limited BBB penetration. Nonetheless, caution is necessary in interpreting these findings due to potential risks of excessive PAH inhibition, especially in phenylketonuria [46].

Further studies should investigate the safety and efficacy of the proposed compound in various dosage settings over time and explore the specificity of the inhibitory effects in extracerebral regions. Despite these limitations, the study suggests the potential of the compound to enhance the efficacy of L-DOPA/Carbidopa combination therapy in Parkinson's's disease treatment.

ACKNOWLEDGEMENTS

The authors would like to thank Ayça Ece Nezir for English language editing.

AUTHOR CONTRIBUTIONS

Concept: H.A., E.S.; Design: H.A., E.S.; Control: H.A., E.S.; Sources: H.A., E.S.; Materials: H.A., E.S.; Data Collection and/or Processing: H.A., E.S.; Analysis and/or Interpretation: H.A., E.S.; Literature Review: H.A., E.S.; Manuscript Writing: H.A., E.S.; Critical Review: H.A., E.S.; Other: -

CONFLICT OF INTEREST

The authors declare that there is no real, potential, or perceived conflict of interest for this article.

ETHICS COMMITTEE APPROVAL

The authors declare that the ethics committee approval is not required for this study.

REFERENCES

1. Gümüş, M., Babacan, Ş.N., Demir, Y., Sert, Y., Koca, İ., Gülçin, İ. (2022). Discovery of sulfadrug-pyrrole conjugates as carbonic anhydrase and acetylcholinesterase inhibitors. Archiv der Pharmazie. 355(1), e2100242. [CrossRef]
2. Reich, S.G., Savitt, J.M. (2019). Parkinson's's Disease. The Medical Clinics of North America, 103(2), 337-350. [CrossRef]
3. Hoehn, M.M., Yahr, M.D. (1967). Parkinson'sism: Onset, progression and mortality. Neurology, 17(5), 427-442. [CrossRef]
4. Cotzias, G.C., Papavasiliou, P.S., Gellene, R. (1969). Modification of Parkinson'sism-chronic treatment with L-dopa. The New England Journal of Medicine, 280(7), 337-345. [CrossRef]
5. Matarazzo, M., Perez-Soriano, A., Stoessl, A.J. (2018). Dyskinesias and levodopa therapy: Why wait? Journal of Neural TransmissionVienna, Austria: 1996, 125(8), 1119-1130. [CrossRef]
6. Yee, R.E., Cheng, D.W., Huang, S.C., Namavari, M., Satyamurthy, N., Barrio, J.R. (2001). Blood-brain barrier and neuronal membrane transport of 6-[^{18}F]fluoro-L-DOPA. Biochemical Pharmacology, 62(10), 1409-1415. [CrossRef]
7. Daidone, F., Montioli, R., Paiardini, A., Cellini, B., Macchiarulo, A., Giardina, G., Bossa, F., Borri Voltattorni, C. (2012). Identification by virtual screening and *in vitro* testing of human DOPA decarboxylase inhibitors. PloS one, 7(2), e31610. [CrossRef]
8. Hoy, S.M. (2019). Levodopa/Carbidopa enteral suspension: A review in advanced Parkinson's Disease. Drugs, 79(15), 1709-1718. [CrossRef]
9. Armstrong, M.J., Okun, M.S. (2020). Diagnosis and treatment of Parkinson's disease: A review. The Journal of the American Medical Association, 323(6), 548-560. [CrossRef]
10. Lees, A., Tolosa, E., Stocchi, F., Ferreira, J.J., Rascol, O., Antonini, A., Poewe, W. (2023). Optimizing levodopa therapy, when and how? Perspectives on the importance of delivery and the potential for an early combination approach. Expert Review of Neurotherapeutics, 23(1), 15-24. [CrossRef]
11. Müller, T. (2020). Pharmacokinetics and pharmacodynamics of levodopa/carbidopa cotherapies for Parkinson's's disease. Expert Opinion on Drug Metabolism Toxicology 16(5), 403-414. [CrossRef]
12. Masood, N., Jimenez-Shahed, J. (2023). Effective management of "OFF" episodes in Parkinson's's Disease: Emerging treatment strategies and unmet clinical needs. Neuropsychiatric Disease Treatment, 19, 247-266. [CrossRef]
13. Antonini, A., Odin, P., Pahwa, R., Aldred, J., Alobaidi, A., Jalundhwala, Y.J., Kukreja, P., Bergmann, L., Inguva, S., Bao, Y., Chaudhuri, K.R. (2021). The long-term impact of Levodopa/Carbidopa intestinal gel on 'off'-time in patients with advanced Parkinson's's Disease: A systematic review. Advances in Theraphy, 38(6), 2854-2890. [CrossRef]
14. Kwon, D.K., Kwatra, M., Wang, J., Ko, H.S. (2022). Levodopa-induced dyskinesia in parkinson's's disease: Pathogenesis and emerging treatment strategies. Cells. 11(23), 3736. [CrossRef]
15. Senek, M., Nielsen, E.I., Nyholm, D. (2017). Levodopa-entacapone-carbidopa intestinal gel in Parkinson's's disease: A randomized crossover study. Movement disorders: Official Journal of the Movement Disorder Society, 32(2), 283–286. [CrossRef]
16. Fitzpatrick P.F. (1999). Tetrahydropterin-dependent amino acid hydroxylases. Annual Review of

Biochemistry, 68, 355-381. [CrossRef]
17. Zurflüh, M.R., Zschocke, J., Lindner, M., Feillet, F., Chery, C., Burlina, A., Stevens, R.C., Thöny, B., Blau, N. (2008). Molecular genetics of tetrahydrobiopterin-responsive phenylalanine hydroxylase deficiency. Human Mutation, 29(1), 167-175. [CrossRef]
18. Butt, S.S., Badshah, Y., Shabbir, M., Rafiq, M. (2020). Molecular docking using chimera and autodock vina software for nonbioinformaticians. JMIR Bioinformatics and Biotechnology, 1(1), e14232. [CrossRef]
19. Kelleci Çelik, F., Karaduman, G. (2023). *In silico* QSAR modeling to predict the safe use of antibiotics during pregnancy. Drug and Chemical Toxicology, 46(5), 962-971. [CrossRef]
20. Kalay, Ş., Akkaya, H. (2023). Molecular modelling of some ligands against acetylcholinesterase to treat Alzheimer's Disease. Journal Research in Pharmacy, 27(6), 2199-2209. [CrossRef]
21. Al-Shabib, N.A., Khan, J.M., Malik, A., Alsenaidy, M.A., Rehman, M.T., AlAjmi, M.F., Alsenaidy, A.M., Husain, F.M., Khan, R.H. (2018). Molecular insight into binding behavior of polyphenol (rutin) with beta lactoglobulin: Spectroscopic, molecular docking and MD simulation studies. Journal of Molecular Liquids, 269, 511-520. [CrossRef]
22. Daina, A., Michielin, O., Zoete, V. (2017). SwissADME: A free web tool to evaluate pharmacokinetics, drug-likeness and medicinal chemistry friendliness of small molecules. Scientific Reports, 7, 42717. [CrossRef]
23. Cheng, F., Li, W., Zhou, Y., Shen, J., Wu, Z., Liu, G., Lee, P.W., Tang, Y. (2012). admetSAR: A comprehensive source and free tool for assessment of chemical ADMET properties. Journal of Chemical Information and Modeling, 52(11), 3099-3105. [CrossRef]
24. Pettersen, E.F., Goddard, T.D., Huang, C.C., Couch, G. ., Greenblatt, D.M., Meng, E.C., Ferrin, T. E. (2004). UCSF Chimera-A visualization system for exploratory research and analysis. Journal of Computational Chemistry, 25(13), 1605-1612. [CrossRef]
25. Goddard, T.D., Huang, C.C., Ferrin, T.E. (2007). Visualizing density maps with UCSF Chimera. Journal of Structural Biology, 157(1), 281-287. [CrossRef]
26. Del Águila Conde, M., Febbraio, F. (2022). Risk assessment of honey bee stressors based on *in silico* analysis of molecular interactions. EFSA Journal, 20(S2), e200912. [CrossRef]
27. Chen, X., Li, H., Tian, L., Li, Q., Luo, J., Zhang, Y. (2020). Analysis of the physicochemical properties of acaricides based on lipinski's rule of five. Journal of Computational Biology, 27(9), 1397-1406. [CrossRef]
28. Sandeep, G., Nagasree, K.P., Hanisha, M., Kumar, M.M. (2011). AUDocker LE: A GUI for virtual screening with AUTODOCK Vina. BMC Research Notes, 4, 445. [CrossRef]
29. Ferreira, L.G., Dos Santos, R.N., Oliva, G., Andricopulo, A.D. (2015). Molecular docking and structure-based drug design strategies. Molecules, 20(7), 13384-13421. [CrossRef]
30. Adasme, M.F., Linnemann, K.L., Bolz, S.N., Kaiser, F., Salentin, S., Haupt, V.J., Schroeder, M. (2021). PLIP 2021: Expanding the scope of the protein-ligand interaction profiler to DNA and RNA. Nucleic Acids Research, 49(W1), W530-W534. [CrossRef]
31. Kremer, J.R., Mastronarde, D.N., McIntosh, J.R. (1996). Computer visualization of three-dimensional image data using IMOD. Journal of Structural Biology, 116(1), 71-76. [CrossRef]
32. Sumera, A.F., Waseem, M., Fatima, A., Malik, N., Ali, A., Zahid, S. (2022). Molecular docking and molecular dynamics studies reveal secretory proteins as novel targets of temozolomide in glioblastoma multiforme. Molecules, 27(21), 7198. [CrossRef]
33. Chao, C.C., Ma, Y.S., Stadtman, E.R. (1997). Modification of protein surface hydrophobicity and methionine oxidation by oxidative systems. Proceedings of the National Academy of Sciences of the United States of America, 94(7), 2969-2974. [CrossRef]
34. Mirmoghtadaie, L., Kadivar, M., Shahedi, M. (2009). Effects of succinylation and deamidation on functional properties of oat protein isolate. Food Chemistry, 2009, 114(1), 127-131. [CrossRef]
35. Sarkar, M., Lu, J., Pielak, G.J. (2014). Protein crowder charge and protein stability. Biochemistry, 53(10), 1601–1606. [CrossRef]
36. Gallivan, J.P., Dougherty, D.A. (1999). Cation-pi interactions in structural biology. Proceedings of the National Academy of Sciences of the United States of America, 96(17), 9459-9464. [CrossRef]
37. Ghosh, P., Bhakta, S., Bhattacharya, M., Sharma, A.R., Sharma, G., Lee, S.S., Chakraborty, C. (2021). A novel multi-epitopic peptide vaccine candidate against *helicobacter pylori*: *In-silico* identification, design, cloning and validation through molecular dynamics. International Journal of Peptide Research and Therapeutics, 27(2), 1149-1166. [CrossRef]
38. López-Blanco, J.R., Aliaga, J.I., Quintana-Ortí, E.S., Chacón, P. (2014). iMODS: Internal coordinates normal mode analysis server. Nucleic Acids Research, 42, W271-W276. [CrossRef]
39. Kovacs, J.A., Chacón, P., Abagyan, R. (2004). Predictions of protein flexibility: First-order measures. Proteins, 56(4), 661-668. [CrossRef]

40. Anandan, S., Gowtham, H.G., Shivakumara, C.S., Thampy, A., Singh, S.B., Murali, M., Shivamallu, C., Pradeep, S., Shilpa, N., Shati, A.A., Alfaifi, M.Y., Elbehairi, S.E.I., Ortega-Castro, J., Frau, J., Flores-Holguín, N., Kollur, S.P., Glossman-Mitnik, D. (2022). Integrated approach for studying bioactive compounds from *Cladosporium* spp. against estrogen receptor alpha as breast cancer drug target. Scientific Reports, 12(1), 22446. [CrossRef]
41. Lipinski, C.A., Lombardo, F., Dominy, B.W., Feeney, P.J. (2001). Experimental and computational approaches to estimate solubility and permeability in drug discovery and development settings. Advanced Drug Delivery Reviews, 1, 46(1-3), 3-26. [CrossRef]
42. Poczta, A., Krzeczyński, P., Tobiasz, J., Rogalska, A., Gajek, A., Marczak, A. (2022). Synthesis and *in vitro* activity of novel melphalan analogs in hematological malignancy cells. International Journal of Molecular Sciences, 23(3), 1760. [CrossRef]
43. Gadaleta, D., Vuković, K., Toma, C., Lavado, G.J., Karmaus, A.L., Mansouri, K., Kleinstreuer, N. C., Benfenati, E., Roncaglioni, A. (2019). SAR and QSAR modeling of a large collection of LD50 rat acute oral toxicity data. Journal of Cheminformatics, 11(1), 58. [CrossRef]
44. Kuoppamäki, M., Korpela, K., Marttila, R., Kaasinen, V., Hartikainen, P., Lyytinen, J., Kaakkola, S., Hänninen, J., Löyttyniemi, E., Kailajärvi, M., Ruokoniemi, P., Ellmén, J. (2009). Comparison of pharmacokinetic profile of levodopa throughout the day between levodopa/carbidopa/ entacapone and levodopa/carbidopa when administered four or five times daily. European Journal of Clinical Pharmacology, 65(5), 443-455. [CrossRef]
45. Erlandsen, H., Flatmark, T., Stevens, R.C., Hough, E. (1998). Crystallographic analysis of the human phenylalanine hydroxylase catalytic domain with bound catechol inhibitors at 2.0 A resolution. Biochemistry, 37(45), 15638-15646. [CrossRef]
46. van Spronsen, F.J., Blau, N., Harding, C., Burlina, A., Longo, N., Bosch, A.M. (2021). Phenylketonuria. Nature Reviews Disease Primers, 7(1), 36. [CrossRef]